

# Effect of Flame Discharge through a Passageway on Rate of Heat Release in IDI Engine

Yoshiharu Ito, Doshisha University  
Jiro Senda, Yanmar Diesel Engine Co., Ltd.  
Hajime Fujimoto, Doshisha University, Karasumaimadegawa, Kamikyoku, Kyoto  
Ko Terada, Nagoya Institut of Technology

## ABSTRACT

This research involved carrying out experiments on an IDI diesel engine fitted with a large swirl chamber. Tests were limited to the conditions on starting and the direction of fuel injection was the test variable; considering injection towards the center of the swirl chamber, injection in the direction of the gas flow and injection in the opposite direction to the gas flow. The phenomena of spray and flame in the swirl chamber were taken using direct and schlieren high speed photography. The two-colour method was used to find data regarding the flame progress through the passageway. Data were subsequently used to attribute the rate of heat release to the main and swirl chambers using the distribution method.

## INTRODUCTION

Generally the analysis of combustion, including particle emission, in diesel engines requires a grasp of state of the combustion, i.e., gas flows in cylinder, spray development, mixing between evaporated gas of fuel and surrounding air etc., as well as of rate of heat release. To data, numerous modellings for rate of heat release have been made for DI engines(1), to the almost complete exclusion of IDI engines. One author(2) suggests a method for cases soluble by pure thermodynamic analysis, whereby, in cases where a negligible pressure difference can be assumed to exist between the main and swirl chambers, the total rate of heat release for both chambers is mathematically distributed to the respective chambers. This calculation requires data regarding the flame development passing through the passageway.

This research was carried out on an IDI air-cooled, 2-cycle diesel engine which, to permit internal visualization, was fitted with a swirl chamber with an exceptionally large volume ratio compared to the main chamber. The purpose was to collect certain data regarding the combustion process. The observations, measurements and calculations listed below were carried out, concentrating on the conditions of the engine at starting with the direction of fuel injection being varied to investigate the effects on gas flows inside the cylinder.

- 1) Observations of flame development using direct and schlieren high speed photography.
- 2) Measurement of flame and spray occupancy rates using projected areas of the same photographs of the combustion chamber.
- 3) Confirmation of the flame presence ratio in the passageway, measurement of flame temperature and flame tip velocity using the two-colour method.
- 4) Calculation of rate of heat release for the main and swirl chambers with the distribution method, using the cylinder pressure measured in the swirl chamber.

## EXPERIMENTAL APPARATUS AND PROCEDURS

The dimentions of the 2-cycle, single-cylinder, IDI air-cooled diesel engine used in this research are listed in Table 1. The engine (bore 85mm, effective stroke 61.1mm), has been fitted with a far langer than normal swirl chamber with a volume ratio of 84.1% compared with the main chamber. This permits visualization of the spray and flame in the swirl chamber and the taking of accurate measurements due to the relatively expanded volume. Furthermore, this engine has the capability of simulating combustion in the cavity of DI engines, which have become increasingly compact in recent years.

This research concentrated on the no-load, constant speed running on starting at  $19.7\text{s}^{-1}$  constant conditions with an excess air ratio of 8.1.

Table 1 Dimensions of used IDI diesel engine

Revolutional speed	$\text{s}^{-1}$	19.7
Cylinder bore	mm	85
Stroke volume	$10^{-3}\text{m}^3$	567
Start of compression	CA(ABDC)	85
Effective stroke	mm	61.1
Effective compression ratio		13.8
Swirl chamber volume ratio	%	84.1
Passageway area ratio	%	1.0

Figure 1 outlines the swirl chamber visualization method and the two colour method for temperature measurement of the flame in the passageway. The swirl chamber (SC) has a diameter of 30mm and a thickness of 20mm and the passageway (PW) a diameter of 10 mm and a length of 43mm. Both sides of the swirl chamber are provided with  $\phi 40\text{mm}$ , 19mm thick observation windows (W) fitted with strengthened glass for direct high speed photography and aluminium silicate glass for schlieren photography. The light sources were a 500W cine lamp for direct high speed photography and a 100W ultra high voltage mercury vapour lamp for schlieren photography with twin concave mirrors used in the normal manner. Kodak 7224 film was used in all cases and maximum filming speed was 8000 frames per second.

Data on the development of the flame in the passageway was obtained through  $\phi 7\text{mm}$ , 2mm thick sapphire glass windows (SW) at  $\phi 4.5\text{mm}$  holes at three points a), b), and c), 38mm, 25mm and 8mm from the main chamber respectively. That is, measurements were taken at three locations; the exit of the swirl chamber, the intermediate point between the main and swirl chambers and at the entrance of the main chamber. The continuous spectrum from the soot particles passed through the measurement holes, aperture A and half-mirror HM and was separated into  $0.520\mu\text{m}$  and  $0.698\mu\text{m}$  wavelengths by the interference filters F1 and F2. Signals from the photo-multiplier detectors PM1 and PM2 then

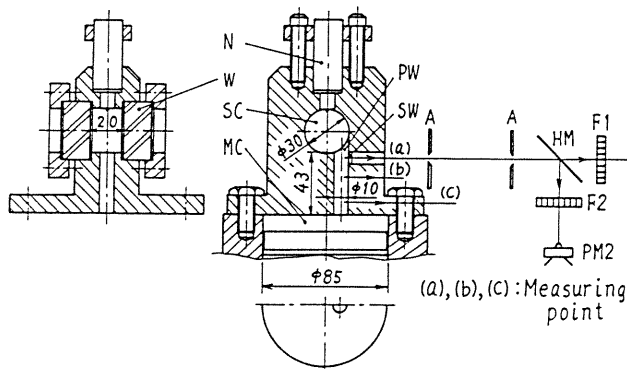


Fig. 1 Detail of swirl chamber and two-colour method

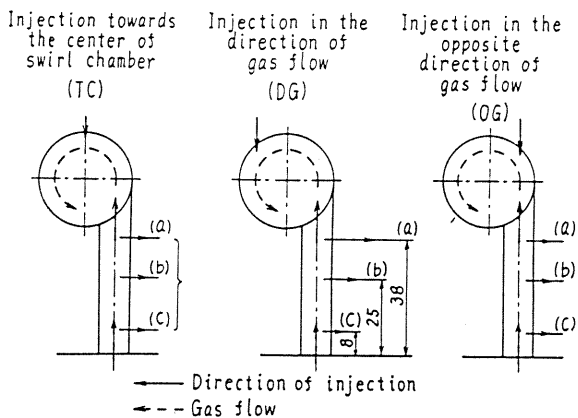


Fig. 2 Relation between direction of injection and gas flow in swirl chamber

underwent statistical processing to determine flame presence rate and calculate the flame temperature and flame tip velocity at the measurement point. Flame presence rate at each point was derived from flow indications as to the presence or lack of flame. The flame tip velocity was calculated from the time it took the flame to reach each measurement point. This velocity means the average and indicates the propagating mechanism of flame transfer from the swirl chamber to the main chamber.

The experimental variables in this research were chosen to observe the effects of fuel distribution in the swirl chamber. As shown in Figure 2, they were fuel injection towards the center of the swirl chamber (DC), injection in the direction of gas flow (DG), and injection in the opposite direction to gas flow (OG). In these cases, the velocities of gas flow in swirl chamber were determined from schlieren photographic images and were found to be approximately 20 m/s near T.D.C.

Nozzle opening pressure was maintained at 7.84 MPa by means of a throttled nozzle (DN4SD24). Test fuel was normal commercial JIS 2 diesel oil. Cylinder pressure necessary to determine rate of heat release was measured using a piezo pressure sensor attached to the swirl chamber side face under the assumption that the pressure loss between the main and swirl chambers was negligible. 100 300 cycle samples were taken for flame data in the passageway and pressure data in the swirl chamber.

#### Rate of Heat Release

To get a view of combustion phenomena in the combustion chamber, it is advantageous to use rate of heat release. This, as well as the corresponding temperature changes, were determined from the pressure changes in the swirl chamber for each experimental variable, calculating for the main and swirl chambers using the distribution method developed by one of our authors (2) which is able to apply for cases where the pressure difference between the main and swirl chamber is small.

Calculation of rate of heat release in both chambers is carried out according to the following distribution procedure:

- 1) Considering the main and swirl chambers to be a single chamber, calculate the total rate of heat release with the swirl chamber pressure.
- 2) From the total heat release, establish the gas composition and characteristics of the gasses in each chamber corresponding to each crank angle.

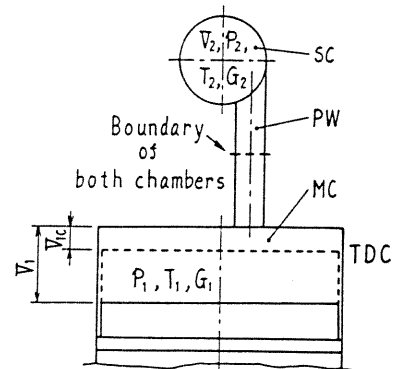


Fig. 3 Division of combustion chamber

3) Distribute the total rate of heat release to the two chambers, under the following assumptions.

(i) Up to the commencement of fuel injection, the two chambers are considered as one and the rate of heat release of the two chambers are considered to be equal to the total rate of heat release.

(ii) Combustion commences in the swirl chamber and is transferred to the main chamber.

(iii) The boundary of the swirl and main chambers is decided, for instance, as shown in Figure 3.

(iv) Up to the commencement of heat release in the main chamber, all heat release is considered to occur only in the swirl chamber. After completion of heat release in the swirl chamber, all heat release is considered to occur only in the main chamber.

(v) At times when combustion is taking place in both chambers simultaneously, heat release is progressing in both chambers. This is divided between the two chambers in proportion to the crank position to determine the respective rate of heat release.

The periods before the commencement of heat release in the main chamber and after completion of heat release in the swirl chamber are important for the distribution of the total rate of heat release between the two chambers. Subsequently, in this research, combustion in the main chamber was defined to have started when the flame presence rate at the measuring points shown in Figure 2 was 50% or more and combustion in the swirl chamber was defined to have been completed when the flame presence ratio was 50% or less. Consequently, calculations were carried out for each measurement point. After the rate of heat release has been determined for each chamber, respective temperature developments were calculated using the Runge-Kuta method. Specific heat of gasses in the combustion chamber were determined using the Edson s(3) temperature fifth order equation for each composition of gas.

The basic equation are as follows:

$$dQ_1 + dI_1 = dU_1 + A p_1 dV_1 \quad (1)$$

$$dQ_2 + dI_2 = dU_2 \quad (2)$$

$$p_1 V_1 = G_1 R_1 T_1 \quad (3)$$

$$p_2 V_2 = G_2 R_2 T_2 \quad (4)$$

$$dI_1 = i_1 dG_1 \text{ when } dI_1 = -dI_2 < 0 \quad (5)$$

$$dI_1 = i_2 dG_1 \text{ when } dI_1 = -dI_2 > 0 \quad (6)$$

$$G = G_1 + G_2, \quad dG_1 = -dG_2 \quad (7)$$

$$V_1 = V_{lc} + \frac{V_h}{2} \{1 - \cos\theta + \frac{r}{4}(1 - \cos 2\theta)\} \quad (8)$$

$$\frac{dV_1}{d\theta} = \frac{V_h}{2} (\sin\theta + \frac{r}{2} \sin 2\theta)$$

$$G_1 = \frac{G}{\frac{R_1 T_1 V_2}{R_2 T_2 V_1} + 1} \quad (9)$$

$$dG_1 = -GV_2 \left( \frac{T_1}{R_2 T_2 V_1} dR_1 + \frac{R_1}{R_2 T_2 V_1} dT_1 - \frac{R_1 T_1}{T_2 V_1 R_2^2} dR_2 - \frac{R_1 T_1}{R_2 V_1 T_2^2} dT_2 - \frac{R_1 T_1}{R_2 T_2 V_2^2} dV_1 \right) / \left( \frac{R_1 T_1 V_2}{R_2 T_2 V_1} + 1 \right)^2$$

$$\frac{dT_1}{d\theta} = \frac{1}{BJ-DH} \left( J \frac{dQ_1}{d\theta} - D \frac{dQ_2}{d\theta} - FJ + DL \right)$$

$$\frac{dT_2}{d\theta} = \frac{1}{BJ-DH} \left( H \frac{dQ_1}{d\theta} - B \frac{dQ_2}{d\theta} - FH + BL \right)$$

$$M_1 = \left[ \left( \frac{1}{i_2} \right) - u_1 \right] / (NR_1 T_1 + 1)^2$$

$$M_2 = \left[ \left( \frac{1}{i_2} \right) - u_2 \right] / (NR_1 T_1 + 1)^2$$

$$N = V_2 / R_2 T_2 V_1$$

$$B = G \left( M_1 NR_1 + \frac{C_{v1}}{NR_1 T_1 + 1} \right)$$

$$H = -GM_2 NR_1$$

$$D = -GM_1 N \frac{R_1 T_1}{T_2}$$

$$J = G \left( \frac{C_{v2}}{1 + \frac{1}{NR_1 T_1}} + M_2 N \frac{R_1 T_1}{T_2} \right)$$

$$F = GM_1 NT_1 \left( \frac{dR_1}{d\theta} - \frac{R_1}{R_2} \frac{dR_2}{d\theta} \right) + \left( Ap - GM_1 N \frac{R_1 T_1}{V_1} \right) \frac{dV_1}{d\theta}$$

$$L = -GM_2 NT_1 \left( \frac{dR_1}{d\theta} - \frac{R_1}{R_2} \frac{dR_2}{d\theta} \right) + GM_2 N \frac{R_1 T_1}{V_1} \frac{dV_1}{d\theta}$$

where:

- A = Mechanical equivalent of heat
- G = Weight of gas
- I = Enthalpy
- i = Enthalpy per unit weight of gas
- l = Length of connecting rod
- p = Pressure
- Q = Heat release
- R = Gas constant
- r = Radius of crank arm
- T = Temperature
- U = Internal energy
- V = Cylinder volume
- V<sub>lc</sub> = Clearance volume
- V<sub>h</sub> = Stroke volume
- θ = Crank angle

Subscript 1 shows the state of main chamber and 2 does the state of swirl chamber.

The fuel used in this calculation is n-tridecane, because the compositions of gas in cylinder must be decided. The rate of heat release dQ/d in both chambers is calculated by equations (1) (9). And then the temperature developments are computed by equations (10).

EXPERIMENTAL RESULTS AND DISCUSSION

Combustion Phenomena

Figure 4 shows examples of direct and schlieren high speed photographs of cases with fuel injection towards the center of the swirl chamber (DC), fuel injection in the direction of gas flow (DG) and fuel injection in the opposite direction to the gas flow (OG). In these cases, the cylinder pressure is 2.6 MPa immediately before heat release and the nozzle opening pressure is 7.84 MPa. The direct and schlieren high speed photographs are not always synchronised.

The spray dispersion pattern have an influence on the subsequent combustion and the spreading of the flame in the combustion chamber have an effect on the rate of heat release. And then the spray and flame occupancy rates,  $S_{OR}$  and  $F_{OR}$ , are defined as the ratio of spray and flame areas on the film to the two-dimensional projected areas of the swirl chamber respectively.

Figure 5 shows  $S_{OR}$  and  $F_{OR}$  obtained from schlieren photograph for gas flows in cases of fuel injection towards the center of the swirl chamber DC, fuel injection in the direction of gas flow DG and fuel injection in the opposite direction to the gas flow OG. In each of these cases, the cylinder pressure at the start of heat release was approximately 3.6 MPa. The cases in this figure have higher cylinder pressures than those shown in Figure 4 and fewer samplings were taken. However, the data in Figure 5 give the good quantitative informations from these above-mentioned qualitative combustion photographs.

In case DC in Figure 4(a), it can be seen from the schlieren photograph that the spray tip impinges on the wall surface in the swirl chamber, although the tip is blown with the gas flowing from the passageway at the beginning of injection. It can be seen that the first flame appears at the envelope of the spray where groups of droplets are drifted accumulated by the gas flow and at the bottom of the swirl chamber. The former state of flame appearance is identical to that described by, for instance, Ogasawara(4) for the case of rapid compression machine. The flame developed to approximately fill the entire chamber, and the matching of gas flows and spray was the best amongst the three cases. It can be seen from Figure 5 that  $S_{OR}$  develops rapidly and that  $F_{OR}$  also develops well.

Furthermore,  $F_{OR}$  returned fasted to zero amongst the three cases.

In the case DG in Figure 4(b), the spray is carried undispersed by the gas flow into the center of the swirl chamber and a large quantity of it adheres to the chamber wall. And  $S_{OR}$  is the smallest amongst the three cases. The first flame appears in the vicinity of the bottom wall of the chamber, and the ignition time is most delayed. The combustion proceeds along the wall and enters the passageway but the flame was not at the longest time after the injection start in these three cases and spread in the center part of the chamber. The total flame occupancy rate  $F_{OR}$  in the DG case was the smallest amongst the three cases considered. Therefore, this case could be

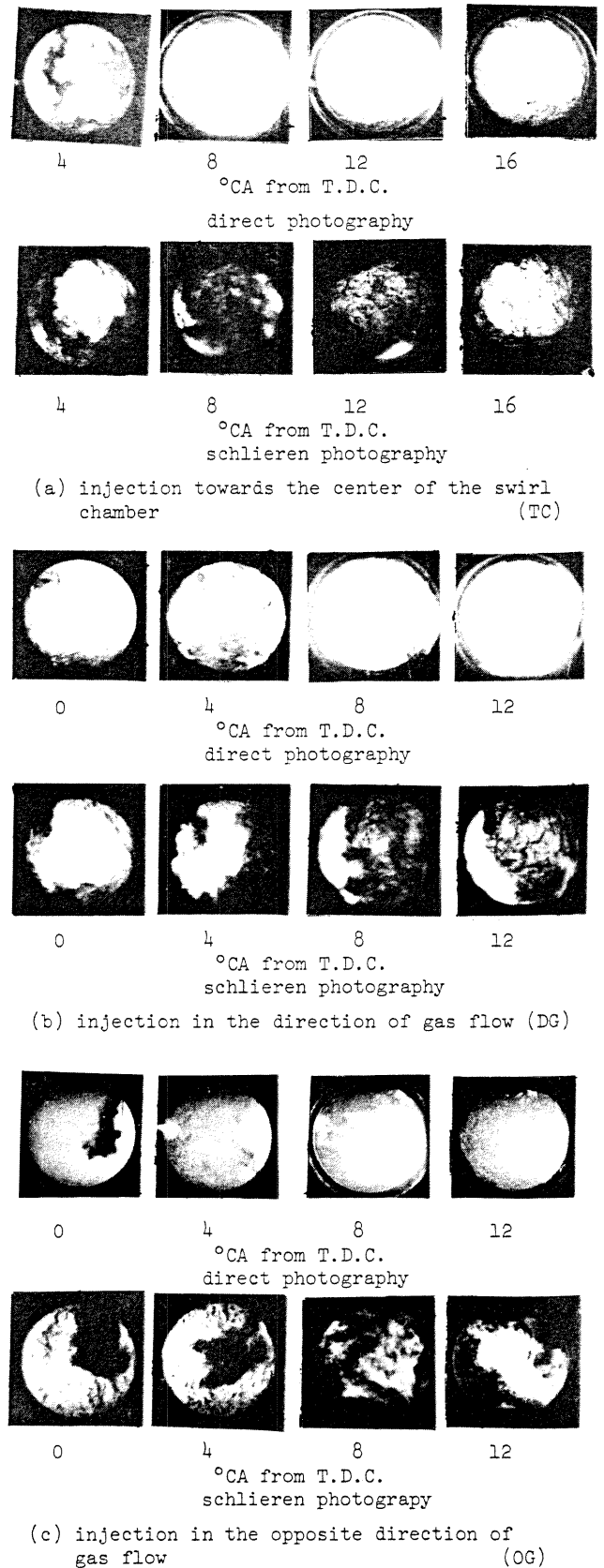


Fig. 4 Combustion phenomena in the swirl chamber

considered to be an over-swirl case. The development of  $S_{OR}$  is sluggish, as can be seen in Figure 5, and consequently  $F_{OR}$  development is small. Furthermore, the period required for  $F_{OR}$  to return to zero is comparatively long compared to case DC.

In the case OG in Figure 4(c), at the early stage of injection when the spray penetration becomes strong in comparison to the gas flow from the passageway, the development pattern of the spray is approximately the same as that in case DC, as can be seen from the  $S_{OR}$  trends in Figure 5. When the gas flow towards the nozzle outlet is stronger, the spray is draw back, as can be seen from the step in the  $S_{OR}$  development curve in Figure 5. Combustion commences in the upper region of the swirl chamber. At the very earliest stage of combustion, the flame exists in this region defined by the mixed gasses but it subsequently spreads throughout the entire chamber due to the effect of the gas flow. Although this case has the slower flame development than that in the case DC, it can be seen from Figure 5 that the  $F_{OR}$  development pattern is approximately the same as that in case DC. And then, due to the influence of the peak in the latter stage of  $S_{OR}$ , there is an apparent tendency for the largest proportion of flame development to occur during the down stroke of the piston, having an adverse effect on the thermal efficiency from a thermodynamic viewpoint.

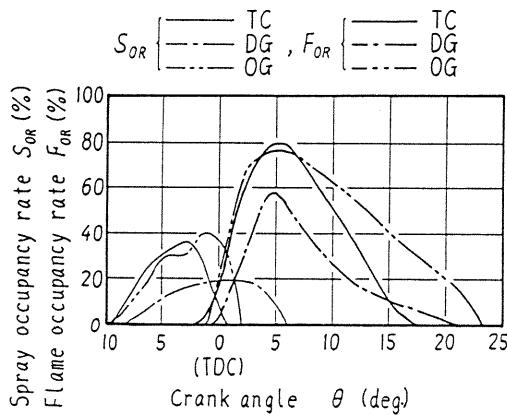


Fig. 5 Spray occupancy rate and flame occupancy rate in swirl chamber

Characteristics of the Flame  
Passing Through the Passageway

Figure 6 shows the flame presence ratio ( $F_{PR}$ ) at each measurement point (a), (b), (c) in the passageway and flame temperature ( $T_{FP}$ ) at the point (a) and Figure 7 the flame tip velocity ( $V_{FT}$ ) passing through the passageway as defined above. (a)-(b), (b)-(c) and (a)-(c) in the Figure 7 refer to the respective intervals between the exit of the swirl chamber (a), the passageway intermediate point (b) and entrance to the main chamber (c).  $V_{FT}$  refers to the average velocity between these points.

As shown in Figure 6, at measuring point (a), the  $F_{PR}$  increases fastest to most rapidly reach complete 100 or near 100% in the fuel injection towards the center of the swirl chamber case (DC), followed by fuel injection in the opposite direction to the gas flow (OG) and fuel injection in the direction of gas flow (DG). The order of risings of these curves at the measuring point (a) corresponds to that of risings of curves for the flame occupancy rate  $F_{OR}$  in Figure 5. The latest rising of  $F_{PR}$  in case DG is brought about by the over-swirl in the swirl chamber observed in Figure 4(b) and the latest appearance of the first flame in three cases. In each of the cases, after the interval where these values are maintained, the flame disappears most rapidly in the case DC. In cases DG and OG, the flame was still present after the crank had passed 20° from T.D.C.. And in case DG, the interval is the longest. The flame temperature  $T_{FP}$  at the measuring point (a) in case

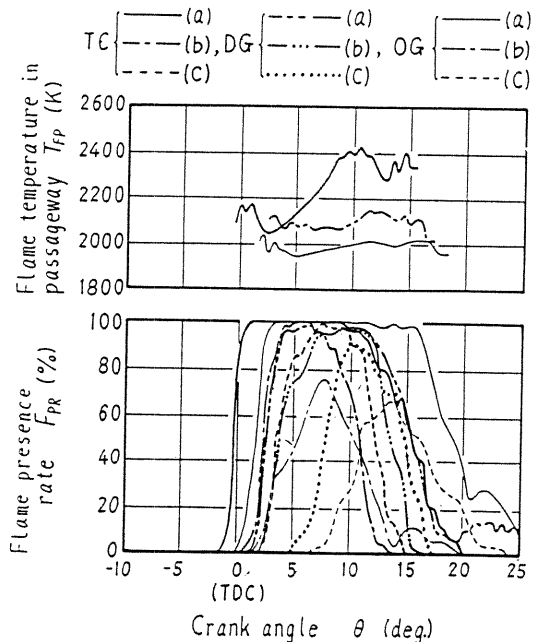


Fig. 6 Flame presence rate and flame temperature in passageway

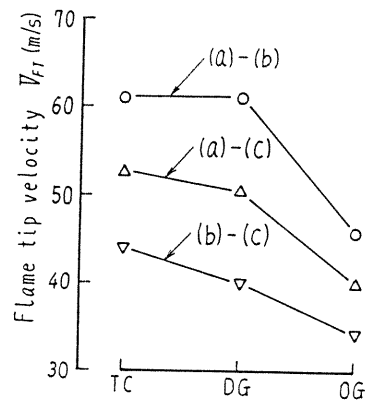


Fig. 7 Flame tip velocity in passageway

DC has the highest value,  $T_{FP}$  in case DG has the middle one and  $T_{FP}$  in case OG gets the lowest one amongst three cases. Case DC is characteristic that the earlier stage of curve  $T_{FP}$  was low and increased as the crank angle progressed. This is due to the smooth development between completion of combustion in the swirl chamber and the flame entering the passageway, as can be seen from the combustion photograph examples given above and flame occupancy rates in Figure 5. Therefore, the gas flow has the appropriateness to the spreading and burning of the spray. In the case DG, the trend of curve of  $T_{FP}$  is caused by the entry of fuel adhered to the wall of swirl chamber into the passageway at latter stage of combustion. In the OG case, it can be seen from the same photographs and Figure 5 that after the flame begins and develops in the upper part of the swirl chamber, it spreads throughout the entire chamber, and then, the main combustion proceeds in the chamber. This is thought to account for the low  $T_{FP}$  in this case.

Approximately the same tendencies as above were observed at measuring point (b) and (c). However, as the measuring points become closer to the entrance to main chamber,  $F_{PR}$  development becomes slower and does not reach the 100% level. This is particularly noticeable from measurements at the entrance to the main chamber in the OG case. This can be considered from the combustion phenomena in the swirl chamber in the same way as above, that is, the flame enters the main chamber after almost all fuel is burned in the swirl chamber at a crank position well after T.D.C..

At all measurement points, the flame tip velocity ( $V_{FT}$ ) was shown to be highest in the case of fuel injection towards the center of the swirl chamber (DC), followed by fuel injection in the direction of gas flow (DG) and fuel injection in the opposite direction to the gas flow (OG). This can also be explained in the same manner from the combustion phenomena. The low  $V_{FT}$  in case OG is mainly due to the progression of flame from the swirl to the main chamber by means of the delayed and sluggish passage of varified combustion in the swirl chamber to the passageway at advanced crank angles noticeable from Figure 5. Low  $V_{FT}$  in all cases between points (b)-(c) is probably due to the resistance and cooling effect of the passageway. It is noteworthy that the value of  $V_{FT}$  of about 60 m/s determined between (a)-(b) in cases DC and DG is approximately equal to both the value determined by Lyn (5) through flame velocity measurements in a compact, high speed DI diesel engine and to that determined by one of our authors through diesel flame growth speed measurements in a constant volume combustion chamber(6).

#### Rate of Heat Release

The rate of heat release and temperature developments obtained using the previously described distribution method on the swirl chamber pressure in the upper part of Figure 8 are represented together in the same Figure. Figure 8(a) represents the case with fuel injection towards the center of the swirl chamber (DC), 8(b)

The case of injection in the direction of gas flow (DG) and 8(c) the case of injection in the opposite direction to gas flow (OG). The heavy solid lines represent the temperature and rate of heat release from the swirl chamber pressure development, i.e. the total rate of heat release. The heavy dashed lines represent the rate of heat release and temperature distributions in the swirl chamber, when the commencement of main chamber combustion and completion of swirl chamber combustion occur at the exit from the swirl chamber, that is, at the measuring point (a). Fine dashed lines represent all developments in the main chamber. Heavy two-dot chain lines represent swirl chamber developments at the time of the start of combustion in the former chamber and the end of combustion in the latter one decided by the information of flame at the intermediate position between the main and swirl chambers, i.e., measuring point (b), and fine two-dot chain lines represent main chamber developments at the time at this position. Heavy broken lines represent swirl chamber developments at the time at the main chamber entrance, i.e., measuring point (c), and fine broken lines represent main chamber developments at the time at this position.

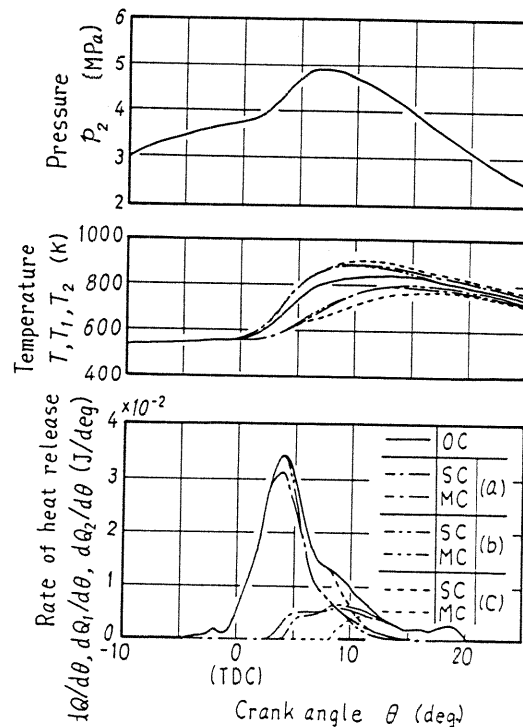
Large variations in the curves of rate of heat release are observed in these Figures for each direction of fuel injection at the different measurement positions where commencement of main chamber combustion and completion of swirl chamber combustion are investigated. This is due to the extremely long passageway (43mm) in comparison to that in standard diesel engines. It is predicted that these variations indicated by our calculations would not occur in standard engines with short passageways. For example, in the case OG the rate of heat release in the main chamber has the almost zero value when the information of flame obtained at the measuring point (c). In consequence, the time measured at point (a) is the best information as for the decision of the start and end of combustion in the swirl and main combustion chamber applying our calculation method for a standard IDI diesel engine.

The periods of heat release are increasingly delayed from the case of fuel injection towards the center of the swirl chamber (DC), the case of injection in the opposite direction of gas flow (OG) to the case of injection in the direction to gas flow (DG) and show remarkable conformity with the flame occupancy rate development periods, shown in Figure 5. The rate of increase in the rate of heat release similarly show remarkable conformity with that of flame occupancy rates shown in Figure 5.

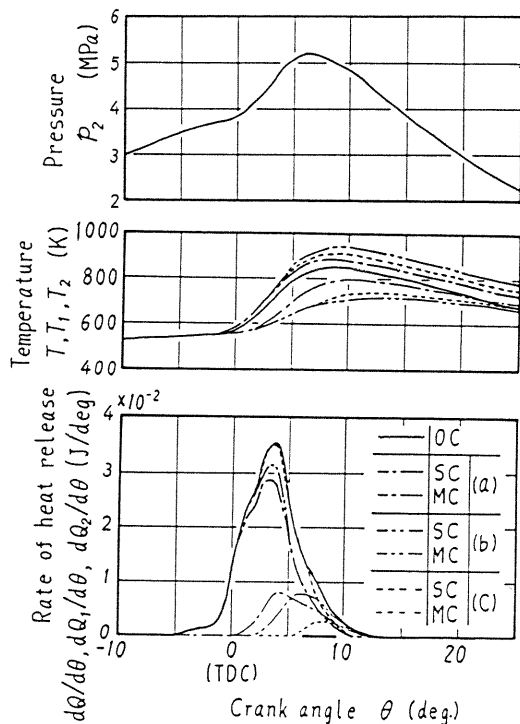
In the OG case, as was described when discussing the flame occupancy rates, the gas flow from the passageway draws the spray back to the nozzle exit. The initial flame develops in this area of spray but subsequently, combustion spreads throughout the entire combustion chamber with the gas flow. This leads to high spread of flame and initial high rate of increase in the rate of heat release, although the first flame appearance was delayed slower than in the case DC. Furthermore, in contrast to the maximum development time in the case of maximum rate of heat release, this case has the minimum development time. As described above, in the initial stages of combustion, the development of the flame occupancy rates and rate

of heat release correspond very closely but differ widely in the latter stages of combustion. Particularly in the OG case, despite increasing flame occupancy rate values, the rate of heat release shows a decreasing trend. The flame presence in this case continues for the longest period of the three fuel injection cases, into the stage when the piston is on its downward stroke and the volume is expanding rapidly. In this period, the flame is confined to the swirl chamber and does not contribute to heat release.

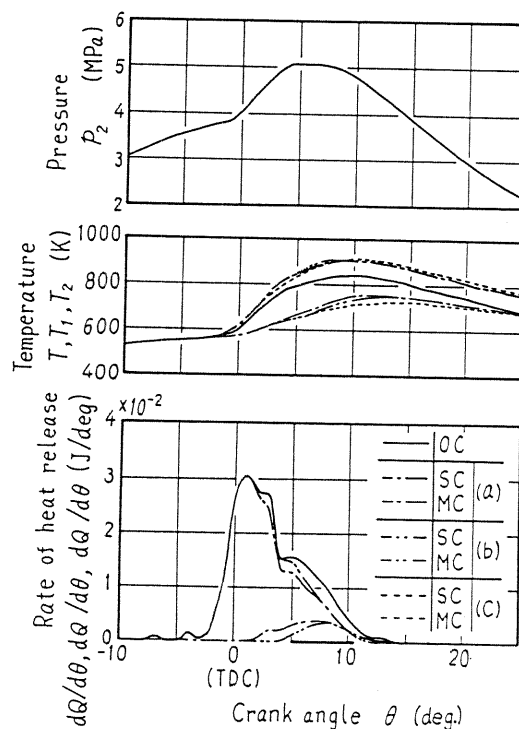
The rate of heat release in the main chamber is decreasing corresponding to the direction of injection, that is, in case DG in that DC and in that OG, as observed on the films in Figure 4. And these rates are smaller than those in the swirl chambers. This is thought to be because the experiment was conducted running only under starting conditions with a high excess air ratio of approximately 8.1. And also, as was outlined under combustion phenomena, the amount of flame entering the passageway was greatest in the case of injection in the direction to gas flow (DG), resulting in the largest heat release in the main chamber, as can be seen from Figure 8(b). The temperature in the swirl chamber is higher than that when both chambers are considered one chamber. This temperature is also higher than that in the main chamber. This is the reason why the main combustion is proceeding in the swirl chamber and a small deal of fuel is burning in the main chamber.



(b) injection in the direction of gas flow (DG)



(a) injection towards the center of the swirl chamber (TC)



(c) injection in the opposite direction of gas flow (OG)

Fig. 8 Pressure, temperature and rate of heat release in swirl chamber and main chamber

## CONCLUSION

The following results were derived from the experiments conducted for this research.

1) The directions of injection have the great influence on the spray and flame developments in the swirl chamber. And these developments bring about the tendencies in the flame presence rate, the flame temperature and the flame tip velocity in the passageway, and the rate of heat release in the swirl and main chambers.

2) Flame temperature through the passageway was found to decrease in order from the case with fuel injection towards the swirl chamber, the case of injection in the direction of gas flow and were slowest in the case of injection in the opposite direction to gas flow.

3) Flame tip velocity at each measuring point in the passageway was slowest in the case of injection in the opposite direction to gas flow.

4) At initial stages of combustion in the swirl chamber, developments of the flame occupancy rates and rate of heat release were found to conform very closely. The periods of commencement of heat release were found to be increasingly delayed from the case with fuel injection towards the center of the swirl chamber, the case of injection in the opposite direction of gas flow to the case of injection in the direction to gas flow.

5) The rates of heat release in the main chamber were found to decrease in order from the case with fuel injection in the direction of gas flow, the case of injection towards the center of the swirl chamber and were lowest in the case of injection in the opposite direction to gas flow due to the amount of flame entered from the swirl chamber to the passageway.

## ACKNOWLEDGEMENTS

The authors would like to offer them sincere thanks to Prof. Hideo Miki, Dr. Kozo Ishida, Mr. Kitaura, Mr. Saito, Mr. Ichiyangi and Mr. Tagaito for their invaluable assistance with this research.

## REFERENCES

- 1) Matsui, Y. and Matsuoka, S.,  
" The Effects of Some Engine Variables on Measured Rates of Air Entrainment and Heat Release in a DI Diesel Engine,"  
SAE Paper, No. 800253, pp. 219-230, 1980.
- 2) Terade, K.,  
" Zur Ermittlung der Heizverläufe in einem Nebenkammer-Dieselmotor,"  
MTZ 40-5, pp. 237-243, 1975.
- 3) Edson, M. H.,  
" The Influence of Compression Ratio and Dissociation on Ideal Otto Cycle Engine Thermal Efficiency,"  
SAE Progress in Technology 7, pp. 49-81, 1964.
- 4) Ogasawara, M., et al.,  
" Photographic Study on the Spray Combustion by Means of a Rapid Compression Machine,"  
Internal Combustion Engine, Vol. 15, NO. 180,  
pp. 9-15 (In Japanese)
- 5) Lyn, W. T.,  
" Study of Burning Rate and Nature of Combustion in Diesel Engine,"  
9th Int. Symposium on Combustion,  
pp. 1069-1082, 1962
- 6) Fujimoto, H., et al.,  
" Investigation on Combustion in Medium-Speed Diesel Engines Using Model Chamber,"  
Proc. 14th CIMAC, pp. D38-1-D38-27, 1981